NUMERICAL INVESTIGATION ON THE DISPERSION OF HYDROGEN LEAKING FROM A HYDROGEN FUEL CELL VEHICLE IN SEABORNE TRANSPORTATION

Hideyuki Oka[1], Yuji Ogata[2], Yasushi Oka[3] and Susumu Ota[4]
[1] Maritime Risk Assessment Department, National Maritime Research Institute, Shinkawa, Mitaka, Tokyo 181-0004, Japan, hoka@nmri.go.jp
[2] Research Institute of Science for Safety and Sustainability, National Institute of Advanced Industrial Science and Technology, 16-1 Onogawa, Tsukuba, Ibaraki 305-8569, Japan, yuji-ogata@aist.go.jp
[3] Faculty of Environment and Information Sciences, Yokohama National University, 79-7, Tokiwadai, Hodogaya-ku, Yokohama, Kanagawa 240-8501, Japan, y-oka@ynu.ac.jp
[4] Centre for International Cooperation, National Maritime Research Institute, Shinkawa, Mitaka, Tokyo 181-0004, Japan, ohta@nmri.go.jp

ABSTRACT

The International Maritime Organization under the United Nations has developed safety requirements for seaborne transportation of hydrogen fuel cell vehicles in consideration of a recent increase in such transportation. Japan has led the development of new regulations in the light of some research outcomes including numerical simulations on hydrogen dispersion in a cargo space of a vehicle carrier in case of accidental leakage of hydrogen from the vehicle. Numerical results indicate that the region of space occupied by flammable hydrogen/air mixture strongly depends on the direction of ventilation openings. These findings have contributed to the development of new international regulations.

1 INTRODUCTION

To prevent global warming, vehicles emitting less greenhouse gases such as gas-electric hybrid cars have been developed so far. Furthermore, hydrogen fuel cell vehicles (HFCVs), which emit no CO_2, have recently been developed as ultimate ecologically-friendly cars. Due to such rising demand for environmental protection, seaborne transportation of HFCVs is highly expected to increase. However, the International Convention for the Safety of Life at Sea (SOLAS) does not provide safety regulations for ships carrying them, since the current SOLAS regulations have been developed based on the carriage of the conventional vehicles with gasoline in their tanks. Taking these circumstance into consideration, Japan invited the International Maritime Organization (IMO), which is a specialized agency of the United Nations, to develop appropriate requirements for carriage of HFCVs and compressed natural gas vehicles (CNGVs). IMO agreed to the proposal by Japan and instructed the Sub-Committee on Fire Protection (FP Sub-Committee) to develop such requirements.

Hydrogen leakage may result from the damage of hydrogen storage tanks or connected pipes, or it may be caused by the activation of safety valves of these tanks. In case of leakage, accumulation of leaked hydrogen near the ceiling in a cargo space may happen, since stiffening members referred to as longitudinal girder, web beams and longitudinal frames act as so-called “smoke barriers”. Such accumulation may lead to the outbreak of accidents such as fire and explosion, so that continuous ventilation in an appropriate way is critical to dilute the concentration of hydrogen in cargo holds.

Currently, an effective power ventilation system is required for closed vehicle spaces by SOLAS regulations. In concrete terms, the ventilation system should have the capacity to handle not less than six times air changes per hour in the corresponding cargo space. It is not obvious whether this requirement is sufficient to generate airflow which can dilute the concentration of hydrogen by its lower flammability limit (LFL) everywhere in the cargo space, because the airflow generation strongly depends upon situations such as structures of cargo spaces and an arrangement of ventilation systems. Thus, so as to clarify necessary regulations for safety seaborne transportation, numerical simulations on hydrogen dispersion in a cargo space of vehicle carriers have been carried out in the hypothetical scenario of accidental leakage of hydrogen from one of HFCVs.

Numerical simulations on the hydrogen dispersion in enclosures with partially openings, such as a residential garage, have been conducted extensively so far as a benchmark problem to evaluate the quality and suitability of a number of computational fluid dynamics (CFD) codes[1, 2]. Among all these CFD codes, the Fire Dynamics Simulator (FDS) [3], which is a freely available, open source software developed by the National Institute of Standarts and Technology (NIST), is used in the present study. FDS has been validated through the comparison with experimental data in partially confined spaces[4, 5]. However, FDS needs to be validated with the corresponding experiments before applying it to hydrogen dispersion simulation in ship cargo spaces with a number of stiffening members on the ceiling under mechanically ventilated conditons.

In order to validate FDS, a series of experiments have been conducted by the large-scale wind tunnel of the National Institute of Advanced Industrial Science and Technology (AIST). This facility is the only explosion-proof wind tunnel in Japan. Time-resolved measurements of hydrogen volume fraction and streamwise wind velocity have been made at multiple heights in the wind tunnel with thin metal plates fixed on the ceiling to take account of the effect of stiffening members acting as "smoke barriers". Then, FDS simulation of the experimental setup is conducted to confirm its validity within computation time suitable for practical use. Finally, numerical analyses on hydrogen dispersion in a full-scale cargo hold of a vehicle carrier are carried out to investigate the effect of ventilation flow on its concentration distribution.

2 EXPERIMENTAL DESCRIPTION

In this section, experimental setup of the wind tunnel investigations is briefly described. A series of wind tunnel experiments have been performed by the explosion-proof wind tunnel at the AIST. The main objective is to provide data for evaluating the prediction accuracy of CFD analyses.

The schematic diagram of this test section is illustrated in Fig. 1. The length, width and height of the test section are 20 m, 3.6 m and 1.8 m, respectively. This tunnel has two fans of an explosion proof type and the maximum airflow speed is 3 m/s. As shown in Fig. 2, metal plates like "smoke barriers" are fixed on the ceiling in the test section so as to simulate a part of a real cargo space of a vehicle carrier. Hereafter, these metal plates are referred to as "thin plates". As illustrated in Fig. 1, the spaces between these thin plates are 4.5 m, and two cases of 450 mm and 600 mm in depth are considered for them. Figure 3 illustrates four hydrogen release nozzles set in the middle area between thin plates. Hydrogen is released from all the nozzles simultaneously. As shown in Fig. 4, except for some cases, metal meshes are plugged into the nozzles to prevent hydrogen from flowing out like a jet. The total release rate of hydrogen from four nozzles is set at 0.120 Nm^3 per minute, the value of which corresponds to the maximum allowable rate of hydrogen leakage in collision tests required by the draft regulations of UN/ECE, TRANS, WP.29. Figure 5 shows locations of hydrogen sensors and release nozzles. For comparison with CFD results, it is desirable to obtain experimental data at a certain number of measured points. Therefore, four hydrogen release nozzles are installed near the wind tunnel ceiling in order to measure noticeable values of concentration under forced flow conditions. In this experiment, the airflow speed and the hydrogen release duration are set at 0.5 m/s and 30 minutes, respectively. In addition, to investigate whether dispersed hydrogen accumulates in the wake region behind the thin plate or not, a series of experiments have been separately conducted in the cases where one or four release nozzles are installed near the wind tunnel floor. For details of experiments under other conditions, refer to the relevant IMO document[6].

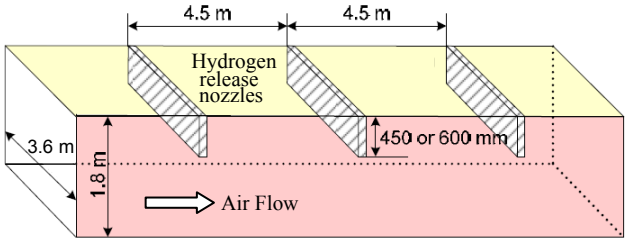

Figure 1. Schematic diagram of the test section in the wind tunnel experiments

Figure 2. Metal plates fixed on the ceiling at a right angle

Figure 6 shows time evolution of hydrogen concentration measured at each sensor position. In the

case of no forced airflow, as shown in Fig. 6(a), the maximum concentration reaches more than 30 vol.% in the last stage during hydrogen release. It is also seen that hydrogen concentrations measured by sensors which are located at positions 1, 4 and 7 are relatively higher than those by the other sensors. These data indicate that the concentration distribution is horizontally stratified in the space between two thin plates. In the case of airflow speed of 0.5 m/s, as shown in Fig. 6(b), the maximum concentration reaches at most 25 vol.%, which is about 20 % less than that in the case of no forced airflow. The stratification of the concentration distribution is also formed in a similar configuration. However, the length of time required for such accumulated hydrogen to dissipate down to the LFL level is more than 50 % shorter than that seen in Fig. 6(a). These results imply that the accumulated hydrogen of relatively high concentration decreases to non-flammable level by means of appropriate ventilation flow.

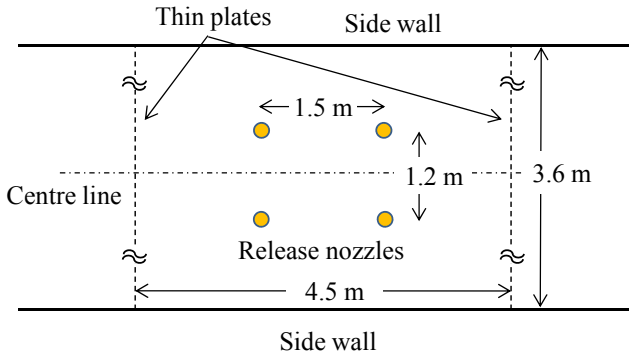

Figure 3. Horizontal location of hydrogen release nozzles

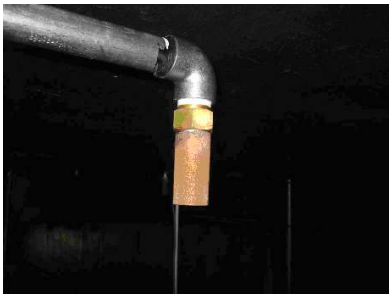

Figure 4. Nozzle with metal mesh

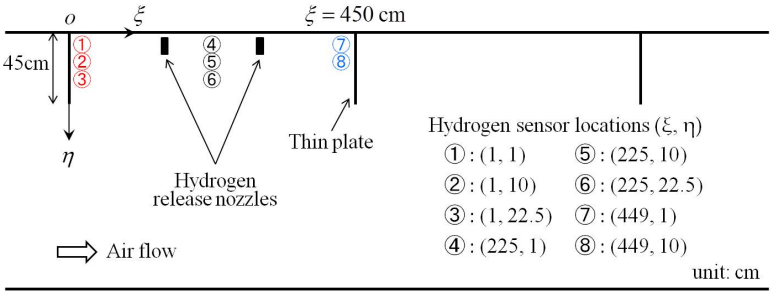

Figure 5. Locations of hydrogen sensors and release nozzles

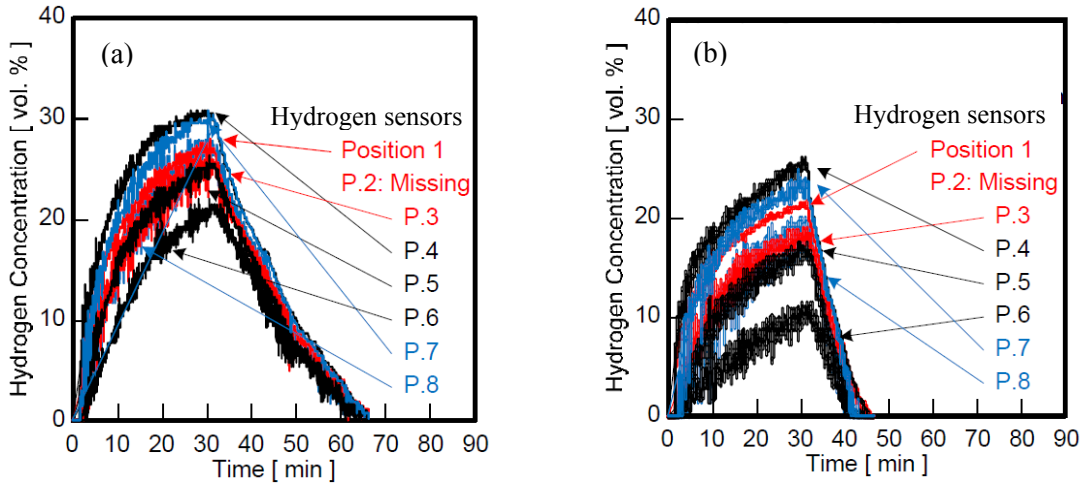

Figure 6. Time evolution of hydrogen concentration at each sensor position: (a) no airflow; (b) wind speed is 0.5 m/s. The depth of thin plates is 0.45 m.

3 COMPUTATIONAL GEOMETRIES AND HYDROGEN RELEASE SCENARIOS

3. 1 Numerical setup of wind tunnel experiment

The wind tunnel experiments described above are numerically simulated by using the NIST Fire Dynamics Simulator (FDS)[3], which is outlined in the next section. Figure 7 shows the computational domain to simulate the experimental setup described in Fig. 1. A Cartesian coordinate system is introduced in such a way that the origin is located on the line of intersection between the tunnel floor and the symmetric plane and that the thin plate in the upstream side is positioned at $x = 0$. To reduce computational costs, the length of the test section in the streamwise direction is set to 15 m instead of 20 m in the real wind tunnel. In addition, a two-dimensional square lattice is taken into consideration to easily simulate realistic turbulence, i.e., velocity fluctuations of airflow[7]. This turbulence generator is positioned at 0.5 m downstream from the inlet boundary. The wind tunnel used in the present study is not a completely closed type, so that airflow fluctuations always exist inside the tunnel. As to hydrogen releases, four nozzles with metal mesh plugs are neglected and simplified to four injection holes embedded on the tunnel ceiling, as illustrated in Fig. 7(b). The CFD calculation is set up to run for 30 minutes. The first 300 seconds allow for the initial transient flow to reach a fully developed flow field. After that, hydrogen is released from these holes into the test section. The simulations are performed on a simple, uniform grid. Three different grid sizes of 2.5, 5 and 9 cm are considered to check the sensitivity to numerical solutions, so that the total number of computational cells are 6,220,800 in the case of the finest grid.

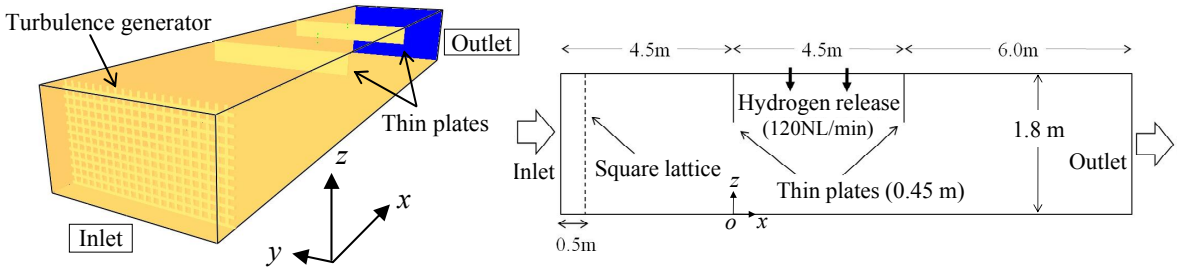

(a) (b)

Figure 7. Numerical setup for the wind tunnel experiments: (a) perspective view of the computational domain; (b) schematic diagram on the symmetric plane ($y = 0$)

3.2 Numerical modeling of cargo space in a vehicle carrier

The numerical analyses are conducted to investigate the effect of ventilation flow on hydrogen behaviour in a cargo space using the same CFD code. A mechanically ventilated cargo space consisting of two gastight decks is considered as a computational domain on the basis of a certain existing vehicle carrier. As shown in Fig. 8(a), the length and width of the computational domain are 44.8 m and 32.26 m, respectively. Longitudinal girders, web beams and longitudinal frames under the ceiling are also taken into consideration. Each depth of T-type girder and web beams is 480 mm and that of L-type frame is 120 mm. These obstructions are modelled as thin metal plates without faceplates in the same way as described earlier. The camber of the deck is neglected in such a way that the height of the computational domain is assumed to be a constant of 2.82 m. Figure 8(b) shows a vehicle model with a very simplified shape, the length, width and height of which are about 4.8 m, 1.8 m and 1.7 m, respectively. Hydrogen is released from surface in red of the small nozzle positioned at the lower part of the model vehicle. The centre of the exit surface is located on the rear side at the height of 0.18 m from the floor. The hydrogen release rate is set at 0.131 Nm^3 per minute. As shown in Fig. 8(b), the hydrogen blows out horizontally towards the fore and aft direction from the exit surface in red. These model vehicles are placed evenly spaced apart in the cargo space as shown in Fig. 8(a). The total number of vehicles placed in the space is 117 and each space between them is set to 0.3 m and 0.1 m in the longitudinal and transverse directions, respectively. The cylindrical objects seen at the upper left and on the lower-right corner are supply and exhaust ducts, respectively.

As to ventilation, it is assumed that air is mechanically supplied and naturally exhausted from

ventilation openings. In Figs. 9(a) and (b), these supply and exhaust openings are shown in red and in light blue, respectively. The size of these openings is 1.4 × 0.8 m, and the height of their centre points is 1.2 m from the floor. Airflow speed at the supply opening is set to 5.8 m/s, which meets the ventilation rate requirement mandated by the SOLAS regulations in such a way that air in the cargo space should be exchanged more than six times per hour. As illustrated in Fig. 10, two different sets of supply and exhaust openings are considered in order to investigate the effect of ventilation flows on distributions of the hydrogen concentration. These configurations of cases A and B can be seen in some of existing vehicle carriers.

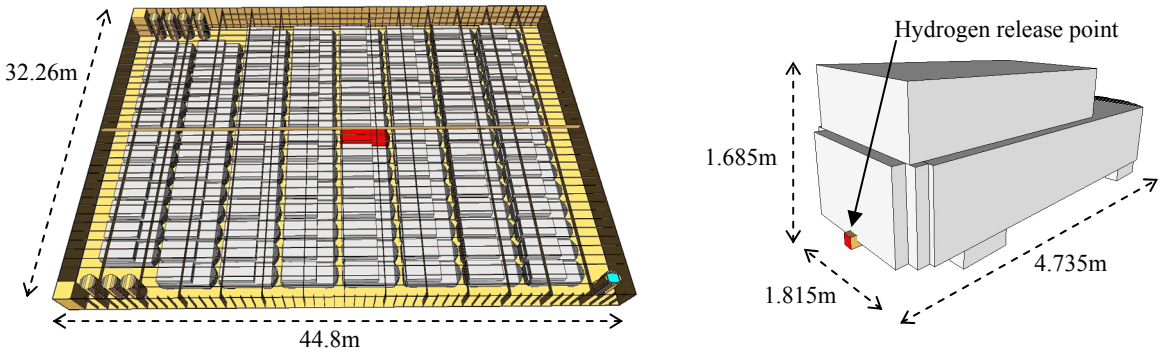

(a) Cargo space model (b) Simplified model of a vehicle

Figure 8. Computational domain and vehicle shape for numerical simulations. 117 vehicles are placed in the cargo space. Hydrogen is released from one of the vehicles, which is shown in red.

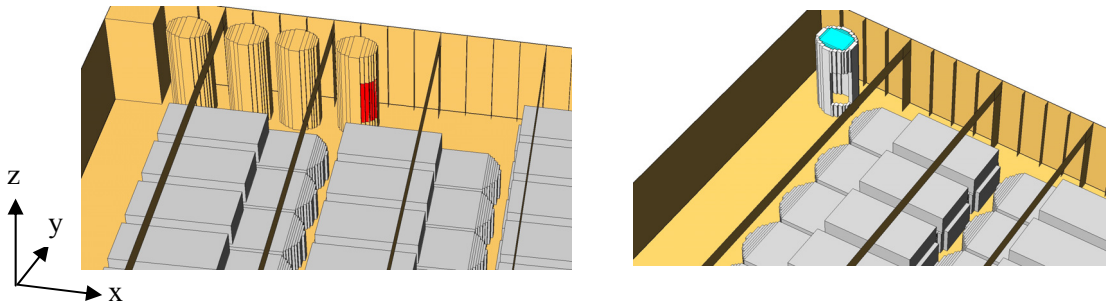

(a) Supply opening (b) Exhaust opening

Figure 9. Supply and exhaust ducts used in the present scenarios. Supply and exhaust openings are indicated in red and light blue in (a) and (b), respectively.

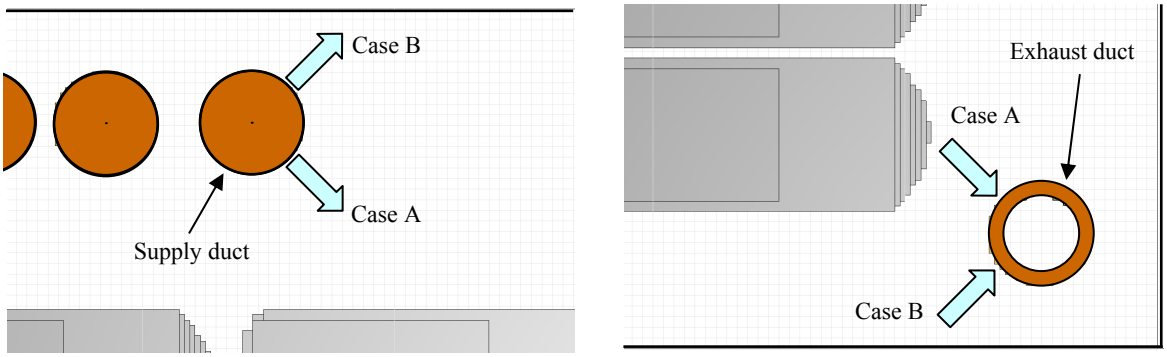

(a) Supply opening (b) Exhaust opening

Figure 10. Two different conditions of ventilation flow directions considered in the present scenarios

The present simulations are performed on a rectilinear grid. The number of grid points used in the computational domain are 360, 256 and 48 in the x, y and z directions, respectively. Hence, each grid size in the horizontal directions is about 0.12 m and the vertical one is about 0.06 m. Two computational cells are assigned to the exit surface of the hydrogen release nozzle, so that the surface area is 0.0144 m^2 and the hydrogen release speed is 0.1625 m/s.

4 NUMERICAL SIMULATION METHOD

Fire Dynamics Simulator (FDS) version 5.5.1[3] is employed in the present simulations. FDS is the most widely used software application as a research and/or engineering tool in the community of fire safety engineering. Various studies of verification and validation have been also conducted to evaluate it in other research fields such as heating, ventilating, and air conditioning (HVAC) [8]. FDS solves the low-Mach number form of the compressible Navier-Stokes equations. The governing equations are the continuity, momentum, mixture fraction, and velocity divergence equations and the ideal gas law, which are numerically solved using a second-order prediction and correction scheme[9]. The details of the model implementation are provided by McGrattan et al. [3]

The turbulence modeling strategy in FDS is based on large eddy simulation (LES). LES requires a sub-grid scale (SGS) model to incorporate unresolved small scale feature of turbulence. By default, the well-recognized Smagorinsky Model (SM) is employed as a SGS model. SM has been widely used in a variety of engineering fields because of its simplicity and high numerical stability. However, SM has an empirical model coefficient C_s, the value of which is not constant and must be changed when applied to different kinds of flow. In addition, the empirical correction of C_s is required in a laminar flow region as well as in the vicinity of solid walls. To resolve this issue, the Coherent Structure Model (CSM)[10] was developed to improve SM and has been used with success in various kinds of turbulent flows[11]. In the present study, therefore, CSM has been incorporated into the source code of FDS version 5.5.1 to overcome the weakness of the default Smagorinsky model. In CSM, its model coefficient is calculated by using a coherent structure function, which is the second invariant in grid-scale flow fields normalized by the magnitude of a velocity gradient tensor. As to the other relevant parameter, the SGS Schmidt number S_{Ct} is set to the default value of 0.5 due to the fact that its small effect on helium dispersion is confirmed[4].

5 RESULTS AND DISCUSSION

5.1 Comparison with wind tunnel experiment

FDS simulation of the experimental setup has been conducted to confirm its validity without the use of extremely fine mesh, since it should be completed within computation time suitable for practical use in this kind of a pragmatic investigation. Instantaneous distributions of velocity and hydrogen concentration fields on the symmetric plane (y = 0) are shown in Figs. 11(a) and (b), respectively. The snapshot of velocity vectors represents a fully developed flow field at the inlet airflow velocity of 0.4 m/s without releasing hydrogen. On the other hand, Figure 11(b) shows the distribution of hydrogen concentration at 30 minutes after it is released into the test section. Unlike in Fig. 11(a), the inlet airflow velocity is set to 0.5 m/s. It is observed that the statistically uniform, approaching flow is obstructed by the first thin plate and consequently a turbulent wake field is formed in the region of space between two thin plates. Since hydrogen is released from four holes on the ceiling into this region, it is very important to accurately simulate the airflow field so as to predict the distributions of hydrogen concentration.

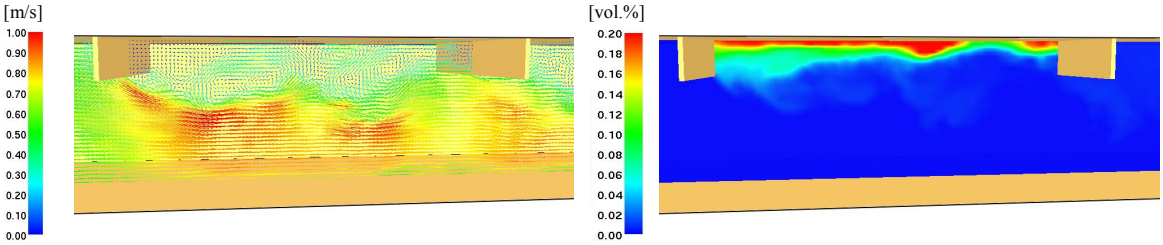

(a) Velocity vectors (b) Hydrogen concentration

Figure 11. Instantaneous distributions of (a) velocity vectors and (b) hydrogen concentration at the symmetric plane (y = 0) in the fully developed flow field

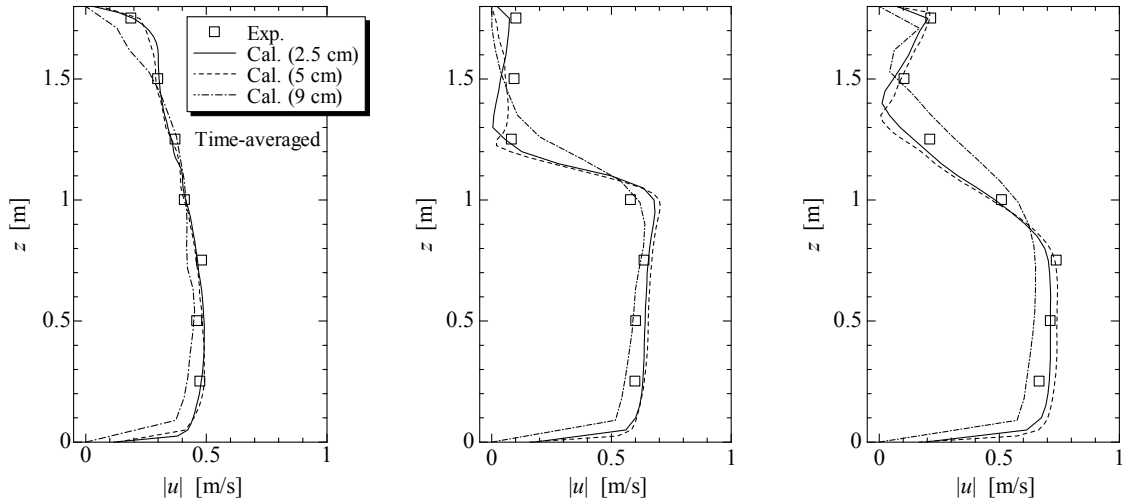

(a) x = -0.5 m (b) x = 0.5 m (c) x = 2.0 m

Figure 12. Vertical profiles of the magnitude of time-averaged, streamwise velocity |u|

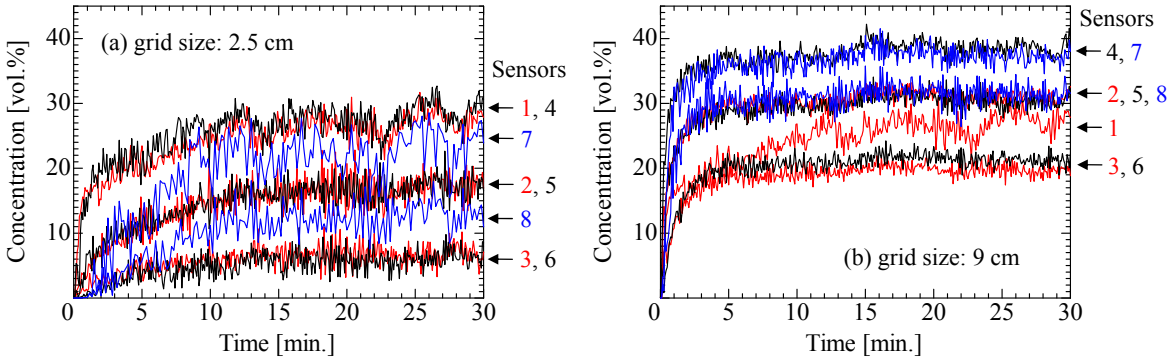

Figure 13. Time evolution of hydrogen concentration at experimental measurement points shown in Fig. 5: (a) grid size is 2.5 cm; (b) grid size is 9 cm

In Fig. 12, numerical results on the airflow velocity are compared with the wind tunnel data. Three vertical profiles of the magnitude of time-averaged, streamwise velocity |u| at x = -0.5, 0.5 and 2 m are shown in Figs. 12(a), (b) and (c), respectively. Results with different grid size are also provided in these figures. It can be seen from this comparison that the present FDS simulation nicely reproduces the experimentally measured data with respect to the airflow field in the wind tunnel in the case where the grid size is smaller than 5 cm. It is also found that the square lattice near the inlet boundary works well as a turbulence generator to make appropriate fluctuations of the inflow velocity. Next, Figure 13 shows time evolution of the hydrogen concentration at the same positions as the experimental measurement points described in Fig. 5. Results with the grid sizes of 2.5 and 9 cm are provided in Figs. 13(a) and (b), respectively. Compared to the measurement data shown in Fig. 6, numerical results with the finest grid roughly reproduce the similar behaviour except two lowest points, i.e., hydrogen sensor positions 3 and 6. The hydrogen concentrations at these two points are considerably underestimated in the present numerical simulation. In consideration of the comparison result of airflow in Fig. 12, these discrepancies might be attributable to poor reproducibility of turbulent flows under strong buoyancy effects. In addition, these differences are probably attributed to simplification of the numerical model of four hydrogen release nozzles. On the other hand, the concentrations at all the measurement points except sensor position 3 are overestimated in Fig. 13(b). In general, numerically obtained flow fluctuations are suppressed in the case of using a coarse computational grid. Therefore, it seems that the released hydrogen accumulates in high concentration near the ceiling.

From the above comparison result, it seems reasonable to conclude that the present FDS simulation can be used for obtaining qualitative information on the relation between ventilation conditions and the resulting profiles of hydrogen concentration when an appropriate computational grid is employed. As described earlier, however, considerably coarse grids are used for simulations on hydrogen dispersion in a full-scale cargo space with forced airflow generated by mechanical ventilation systems due to the restriction of our computer resources.

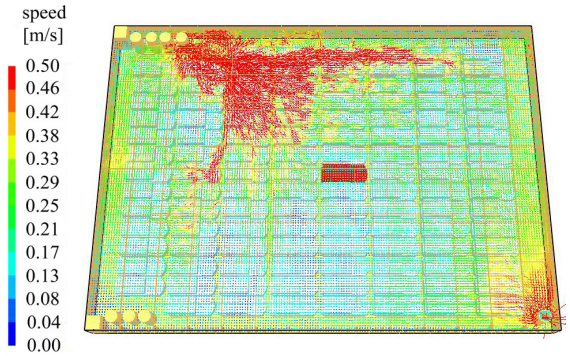

10 minutes later

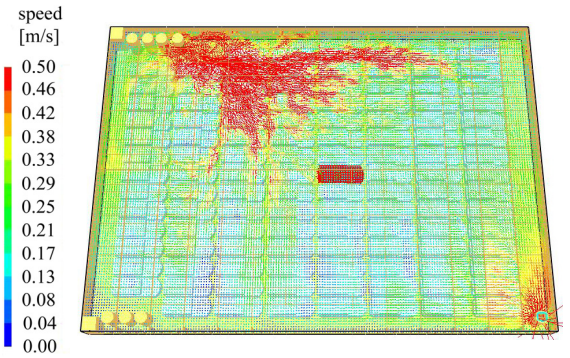

30 minutes later

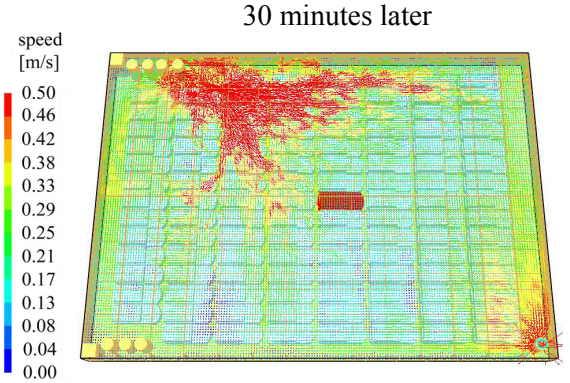

50 minutes later

Figure 14. Time evolution of airflow velocity at 2.0 m in height at 10, 30 and 50 minutes after starting mechanical ventilation in Case A

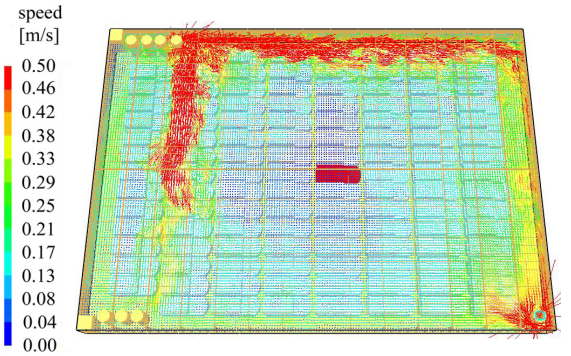

10 minutes later

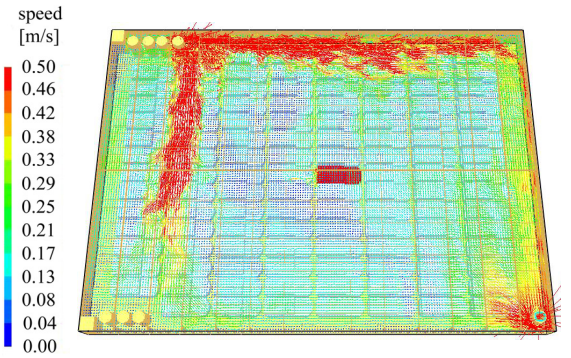

30 minutes later

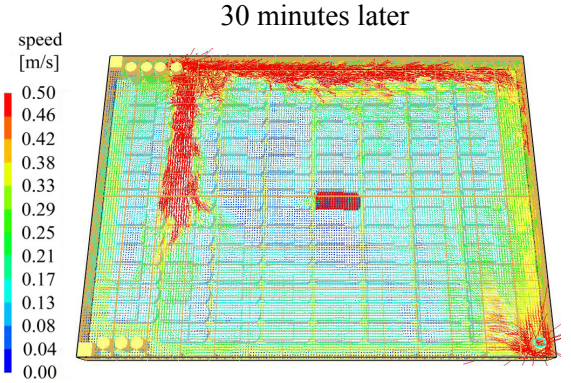

50 minutes later

Figure 15. Time evolution of airflow velocity at 2.0 m in height at 10, 30 and 50 minutes after starting mechanical ventilation in Case B

5.2 Ventilation flow effect in ship cargo space

5.2.1 Ventilation flow

Figure 14 shows the air velocity distributions at 2.0 m in height at 10, 30 and 50 minutes after starting mechanical ventilation in Case A. The velocity vectors are plotted at every three mesh in both directions, and the vectors in red indicate that their magnitude is more than or equal to 0.5 m/s. At this height, the vehicles and thin plates such as the girders and the web beams at the ceiling do

not obstruct the airflow. Hence, it can be observed that roughly speaking, the main stream of such ventilation flow is formed in the direction from top left to right bottom, that is, from the supply duct to the exhaust duct. As to Case B, on the other hand, it can be seen from Fig. 15 that the region of space where the airflow speed is around 0.5 m/s at the same height and time as in Case A is formed in the transverse direction across the cargo space and in the longitudinal direction along the side wall. Results indicate that regardless of these ventilation patterns of Cases A and B, the airflow field in the cargo space becomes almost fully developed within 10 minutes. Therefore, it is reasonable to release hydrogen at 10 minutes after starting the mechanical ventilation so as to avoid initially developing flow effects on hydrogen dispersion.

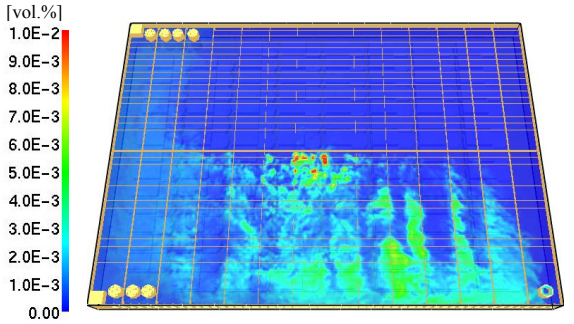

10 minutes later

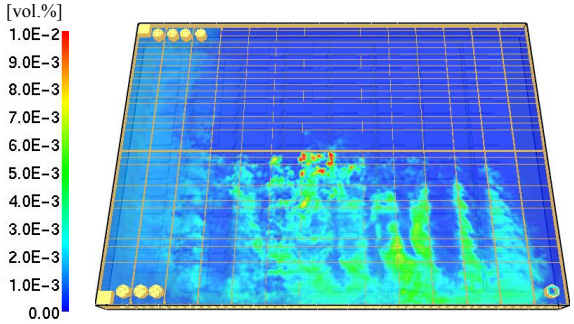

30 minutes later

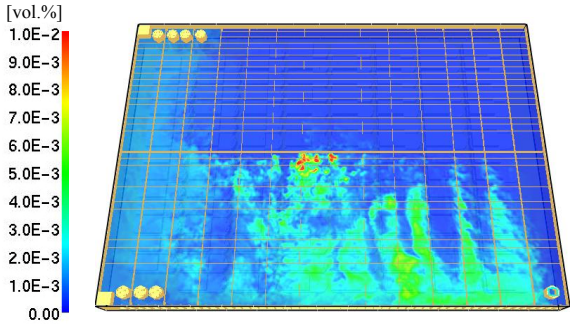

50 minutes later

Figure 16. Hydrogen concentration at 2.0 m in height at 10, 30 and 50 minutes after hydrogen release in Case A

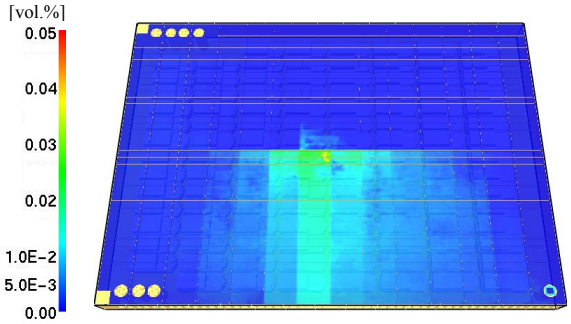

10 minutes later

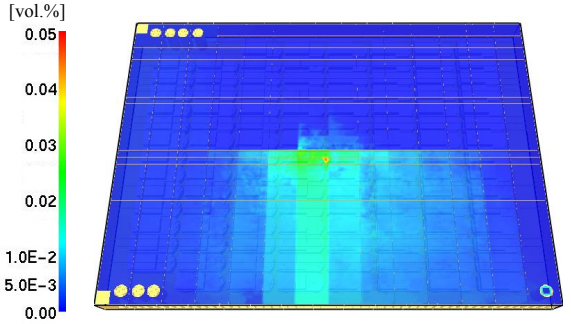

30 minutes later

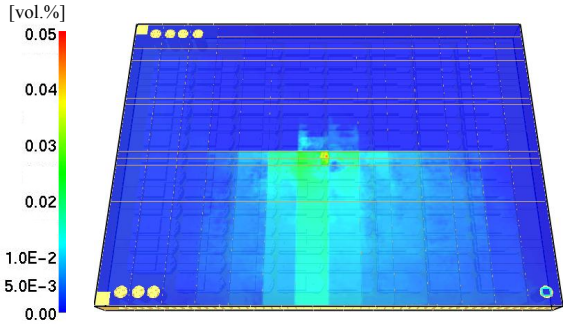

50 minutes later

Figure 17. Hydrogen concentration at 2.76 m in height at 10, 30 and 50 minutes after hydrogen release in Case A

5.2.2 Hydrogen concentration

Figure 16 shows distributions of the hydrogen concentration at the height of 2.0 m at 10, 30 and 50 minutes after releasing hydrogen, that is, 20, 40 and 60 minutes after starting mechanical ventilation in the pattern of Case A. The regions where hydrogen concentration is not less than 1 % are indicated in red. These distribution profiles of hydrogen concentration are almost similar on the whole, though local differences are observed at each time due to the velocity fluctuation. As is the case with the velocity field, the concentration field in the cargo space becomes almost fully developed within 10 minutes. Likewise, such fully developed concentration fields at the height of

2.76 m are shown in Fig. 17. In these figures, the regions where hydrogen concentration is not less than 5 % are indicated in red. It is also observed that the distribution profiles of hydrogen concentration are strongly influenced by the existence of thin plates. Though some amount of released hydrogen rises to the same height as the space surrounded by these thin plates, it seems that there is not any region where the concentration is more than or equal to the lower flammability limit (LFL) under the present calculation conditions. To confirm it from another point of view, iso-surfaces of the hydrogen concentration of 4 %, that is, the lower flammability limit are shown in Fig. 18. It is observed that the hydrogen with relatively high concentration does not reach the ceiling and the spaces where the concentration is not less than the LFL are limited just above the rear side of the vehicle from which hydrogen is released.

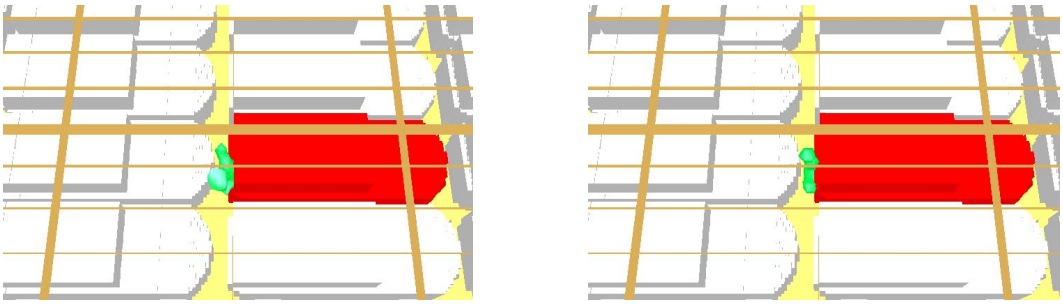

30 minutes later 50 minutes later

Figure 18. Iso-surfaces of LFL concentration of hydrogen/air mixture at 30 and 50 minutes after hydrogen release in Case A

Next, numerical simulations on the hydrogen dispersion in the ventilation pattern of Case B are carried out so as to examine the effect of the direction of ventilation openings. Figure 19 shows snapshots of the hydrogen concentration field at the height of 2.0 m at 30 and 50 minutes after releasing hydrogen. In the same manner as in Case A, the regions where the hydrogen concentration is not less than 1 % are indicated in red. Unlike in Case A, the distribution profile of the hydrogen concentration at 10 minutes is somewhat different from those at 30 and 50 minutes since it is still in the transient process to reach the fully developed state. Likewise, such differences are observed at 2.76 m in height, as provided in Fig. 20. The regions shown in red correspond to not less than 5 % of the hydrogen concentration. These regions of space occupied by relatively higher concentration are much wider than those in Case A. In particular, the flammable hydrogen/air mixture is locally observed on the horizontal plane of 2.76 m in height, even though the existence of such gas is limited in the vicinity of the ceiling above the rear side of the vehicle. The difference in hydrogen concentration between Cases A and B is obviously attributed to whether airflow at a velocity sufficient to dilute the concentration of hydrogen are generated or not around the vehicle from which hydrogen is released. Figure 21 shows iso-surfaces of the LFL concentration to provide a three-dimensional representation of the regions of space occupied by the flammable hydrogen/air mixture. It is observed that a small amount of such mixture gas exists in the regions of space surrounded by thin plates. Therefore, it is found that the direction of ventilation openings is critical to prevent the combustible gas mixture from stagnating near the ceiling even in the case where the ventilation capacity fulfills the current SOLAS regulation.

6 CONCLUDING REMARKS

In this study, in case of accidental leakage of hydrogen from one of HFCVs, numerical simulations on hydrogen dispersion in a full-scale cargo hold of a vehicle carrier have been carried out to investigate the effect of ventilation flow on the distribution of hydrogen concentration. FDS version 5.5.1 with a modification of incorporating the coherent-structure SGS model[10] is employed in the present study. In order to validate FDS, a series of experiments on hydrogen dispersion have been conducted by the large-scale wind tunnel with thin plates fixed on the ceiling to simulate a part of a cargo hold of a vehicle carrier. Measurement data on hydrogen volume fraction and streamwise wind velocity have been compared with CFD results by FDS. Consequently, FDS simulations have qualitatively reproduced these experimental data under the condition that computational grids with an appropriate size are employed.

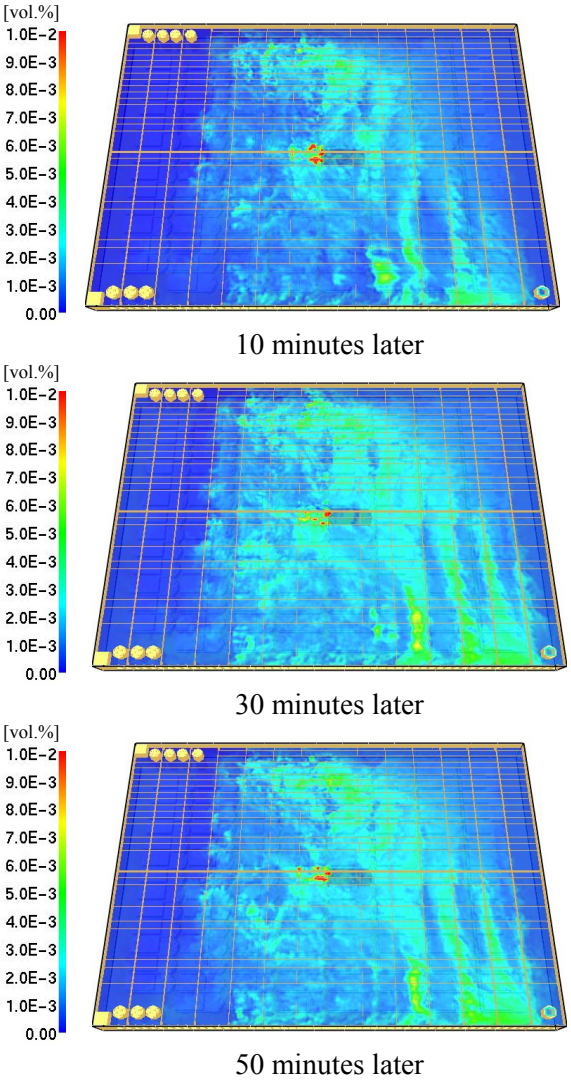

Figure 19. Hydrogen concentration at 2.0 m in height at 10, 30 and 50 minutes after hydrogen release in Case B

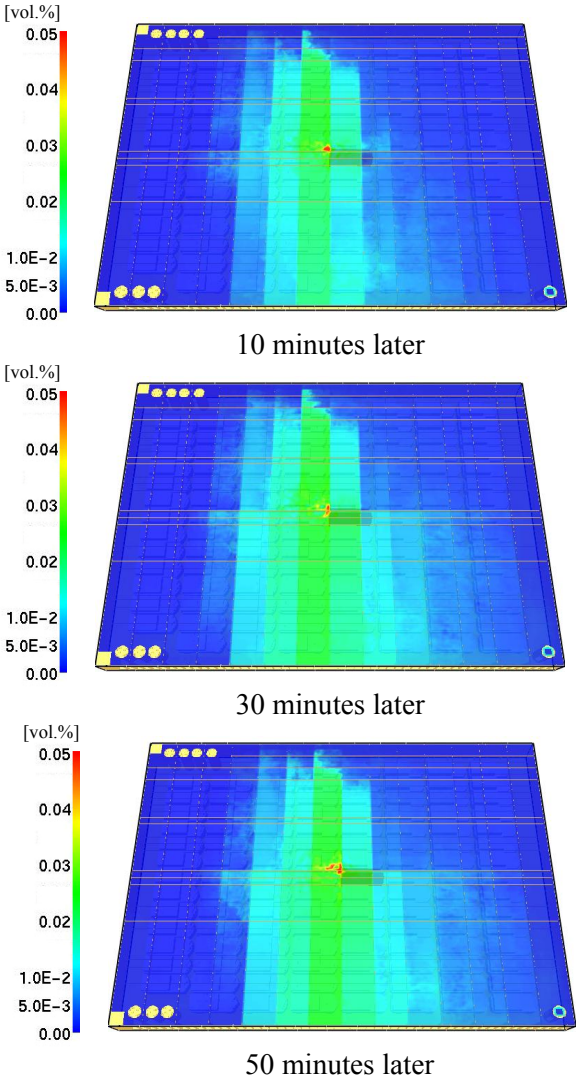

Figure 20. Hydrogen concentration at 2.76 m in height at 10, 30 and 50 minutes after hydrogen release in Case B

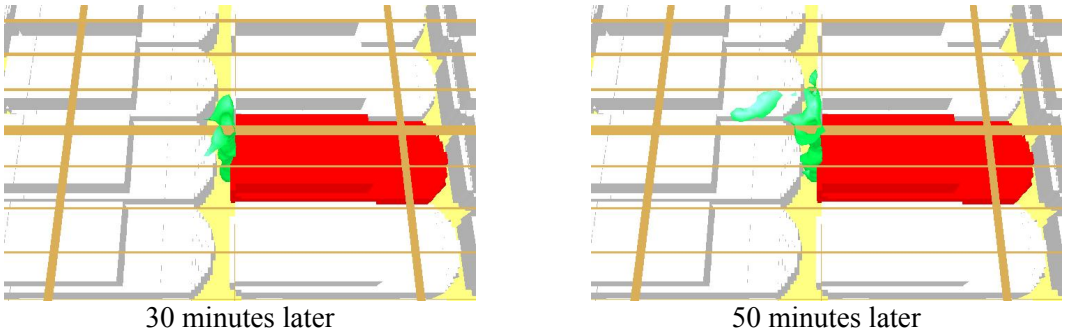

Figure 21. Iso-surfaces of LFL concentration of hydrogen/air mixture at 30 and 50 minutes after hydrogen release in Case B

Next, numerical analyses on hydrogen dispersion inside a full-scale cargo space have been conducted with a focus on the relation between ventilation flows and hydrogen concentration distributions in the region of space surrounded by stiffening members near the ceiling. Through

comparison of two ventilation flow patterns, it has been found that the region of space occupied by flammable hydrogen/air mixture strongly depends on the direction of ventilation openings even in the case where the ventilation capacity fulfills the current SOLAS regulation. However, it seems that the concentration of the dispersed hydrogen does not become so high as to cause extensive overpressure even in case of ignition. These findings have led the IMO's Sub-Committee on Fire Protection to the development of new requirements for the elimination of ignition sources, but not to the development of any new requirement for ventilation since it is not practical to specify details of duct openings. Then, the Sub-Committee has prepared the draft amendments to the SOLAS Convention. Finally, the Maritime Safety Committee of the IMO has adopted the draft amendments, and these new requirements will enter into force at the beginning of year 2016.

ACKNOWLEDGEMENT

This work was carried out as a part of the Japan Ship Technology Research Association (JSTRA) project “Safety study on Seaborne Carriage of Hydrogen Fuel Cell Vehicles” with a financial support by the Nippon Foundation. The authors are deeply indebted to JSTRA and the Nippon Foundation.

REFERENCES

1. Venetsanos, A.G., Papanikolaou, E., Delichatsios, M., Garcia, J., Hansen, O.R., Heitsch, M., Huser, A., Jahn, W., Jordan, T., Lacome, J.-M., Ledin, H.S., Makarov, D., Middha, P., Studer, E., Tchouvelev, A.V., Teodorczyk, A., Verbecke, F. and Van der Voort, M.M., An Inter-Comparison Exercise on the Capabilities of CFD Models to Predict the Short and Long Term Distribution and Mixing of Hydrogen in a Garage, *International Journal of Hydrogen Energy*, **34**, No. 14, 2009, pp. 5912-5923.
2. Papanikolaou, E.A., Venetsanos, A.G., Heitsch, M., Baraldi, D., Huser, A., Pujol, J., Garcia, J. and Markatos, N., HySafe SBEP-V20: Numerical Studies of Release Experiments Inside a Naturally Ventilated Residential Garage, *International Journal of Hydrogen Energy*, **35**, No. 10, 2010, pp. 4747-4757.
3. McGrattan, K., Hostikka, S., Floyd, J., Baum, H., Rehm, R., Mell, W. and McDermott, R., Fire Dynamics Simulator (Version 5) Technical Reference Guide, Volume 1: Mathematical Model, NIST Special Publication 1018-5, 2007.
4. Prasad, K., Pitts, W.M. and Yang, J.C., A Numerical Study of the Release and Dispersion of a Buoyant Gas in Partially Confined Spaces, *International Journal of Hydrogen Energy*, **36**, No. 8, 2011, pp. 5200-5210.
5. Matsuura, K., Nakano, M. and Ishimoto, J., Sensing-Based Risk Mitigation Control of Hydrogen Dispersion and Accumulation in a Partially Open Space with Low-Height Openings by Forced Ventilation, *International Journal of Hydrogen Energy*, **37**, 2012, pp. 1972-1984.
6. Ota, S. and Ogata, Y., Wind Tunnel Experiment on Concentration of Hydrogen in Relation to Airflow Speed, International Maritime Organization document FP55/INF.2 Annex 3, 2011.
7. Ooida, J. and Kuwahara, K., Implicit LES of Turbulence Generated by a Lattice, 16th AIAA Computational Fluid Dynamics Conference, Orlando, Florida, AIAA paper 03-4097, 2003.
8. Musser, A. and McGrattan, K., Evaluation of a Fast Large-Eddy-Simulation Model for Indoor Airflows, *Journal of Architectural Engineering*, **8**, No. 1, 2002, pp. 10-18
9. McDermott, R.J., A Velocity Divergence Constraint for Large-Eddy Simulation of Low Mach Number Flows, *Journal of Computational Physics*, **274**, 2014, pp. 413-431.
10. Kobayashi, H., The Subgrid-Scale Models based on Coherent Structures for Rotating Homogeneous Turbulence and Turbulent Channel Flow, *Physics of Fluids*, **17**, 2005, 045104.
11. Kobayashi, H., Ham, F. and Wu, X., Application of a Local SGS Model Based on Coherent Structures to Complex Geometries, *International Journal of Heat and Fluid Flow*, **29**, 2008, pp. 640-653.